Investigating Creep of Intervertebral Discs under Axial Compression

Subjects: Mechanics

Contributor: Weiqiang Liu , Mengying Yang , Dingding Xiang , Wang Song

Creep responses of intervertebral discs (IVDs) are essential for spinal biomechanics clarification. Yet, there still lacks a well-recognized investigation protocol for this phenomenon. Researchers aim at providing an overview of the in vitro creep tests reported by previous studies, specifically specimen species, testing environment, loading regimes and major results, based on which a preliminary consensus that may guide future creep studies is proposed. Specimens used in creep studies can be simplified as a “bone–disc–bone” structure where three mathematical models can be adopted for describing IVDs’ responses. The preload of 10–50 N for 30 min or three cycles followed by 4 h-creep under constant compression is recommended for ex vivo simulation of physiological condition of long-time sitting or lying. It is worth noticing that species of specimens, environment temperature and humidity all have influences on biomechanical behaviors, and thus are summarized and compared. All factors should be carefully set according to a guideline before tests are conducted to urge comparable results across studies. To this end, researchers also provide a guideline, as mentioned before, and specific steps that might facilitate the community of biomechanics to obtain more repeatable and comparable results from both natural specimens and novel biomaterials.

intervertebral disc creep in vitro mechanical testing biomechanics

1. Introduction

Creep is a time-dependent response of IVD and is a typical feature of viscoelastic materials. In 1982, Twomey et al. [1] defined creep as the progressive deformation of a structure under the constant load when the materials are stressed below their fracture thresholds. One of the most intuitive phenomena, which suggests the formation of creep is that the human body has a height change of 1–2 cm per day [2][3]. To date, several studies described the creep behaviors of the spine under axial compression [4][5][6][7][8][9][10][11][12][13][14][15][16][17]. These investigations highlighted the non-linear and time-dependent behaviors of natural IVDs, showing a rapid decrease in axial height after early compression followed by a slow decrease until reaching equilibrium. Nevertheless, a normalized loading protocol is not yet available to which every study adheres, thus resulting in a significant challenge in comparing mechanical results across studies and hampering the development and testing of biomaterials used for spinal implants [18][19].

2. Factors That Can Influence the Mechanical Properties of IVDs

2.1. Species

2.1.1. Difference in Geometry

The geometry of animals and human IVDs varies, and thus should be taken into consideration. Geometric parameters from various animals' IVDs have been previously measured [20][21][22][23][24], including baboon, sheep, rabbit, rat, mouse and bovine in terms of height, lateral width, anterior–posterior width (AP width) and area. According to the results, human lumbar specimens were larger than all of the aforementioned animal specimens. The value of normalized AP width, which was scaled by the lateral width, was 0.665 for human lumbar discs, and the normalized AP widths for baboon, sheep and mouse lumbar discs were close to human lumbar discs, indicating the similar shapes of those animals' discs with the human lumbar discs, which were all like 'kidney bean'.

2.1.2. Difference in Glycosaminoglycan (GAG) and Water Content

The amount and distribution of GAG in IVDs are functionally important to define swelling pressure, water content and compressive properties [25][26][27]. Generally speaking, GAG and water analysis of specific regions indicate a similar trend, featuring higher GAG and water content levels in the nucleus pulpous (NP) and lower amounts of GAG and water in the annulus fibrosus (AF) [28][29][30]. In addition, GAG and water content were significantly different across species. According to results from Jesse et al. [23], GAG contents in NP of IVDs from calf, porcine, sheep, rabbit, rat and cow tail were similar to those of human species (466 ± 205 μg/mg). GAG contents in AF of IVDs from calf, baboon, rabbit, cow tail indicated approximately the same or higher content with AF from human species (269 μg/mg). The water content of calf, porcine, baboon, sheep, rabbit, rat lumbar, cow tail and rat tail IVDs was similar to that of human in the NP and AF, which were 81% and 76% separately.

2.1.3. Difference in Axial Compressive Mechanics

Jesse et al. [23] conducted experiments to acquire the axial compressive mechanical parameters, including stiffness, range of motion (ROM), step and creep displacement using IVDs from various animals under the same loading protocol (cyclic loading followed by creep test under 0.48 MPa for 1 h), and revealed the impact of species related factors (GAG content, water content and size) on IVDs biomechanics. Their study concluded that the compressive stiffness of the baboon (1426 ± 382 N/mm) and sheep lumbar discs (1432 ± 334 N/mm) was closed to that of humans (1734 ± 446 N/mm). The ROM of cow tails (1.24 ± 0.31 mm) was most similar to that of humans (1.21 ± 0.18 mm). The step displacement of cow tail (1.45 ±0.60 mm) was closed to that of humans (0.90 ± 0.12 mm). The creep displacement of porcine (0.55 ± 0.18 mm), baboon (0.36 ± 0.11 mm), sheep (0.24 ± 0.03 mm), rabbit (0.47 ± 0.17 mm), rat lumbar (0.19 ± 0.02 mm), rat tail (0.40 ± 0.11 mm) was similar to that of humans (0.55 ± 0.03 mm). Their study further demonstrated that axial mechanics of IVDs were similar across species, indicating that the values between species were comparable by altering the load magnitude. In experiments simulating disc herniation, sheep IVDs are good choices with a similar shape to human lumbar IVDs and also herniated at the posterolateral region [31][32]. Large animal models (sheep, ovine, pigs) are suitable for investigating effects of mechanical factors, implant preclinical trials and surgical techniques on biomechanics, while small animal models (rat, mouse) are suitable for studying biological processes. When IVD pressure is of focus, animal models with a

smaller cross-sectional area than human IVDs can be used, and the applied load needs to be changed proportionately [33][34].

2.2. Specimen Harvesting and Storage

Specimens of in vitro creep tests should be carefully processed into bone–disc–bone structures by making parallel cuts at the upper and lower vertebral bones with a distance of ~10 mm from the IVD using a bone saw under aseptic conditions. The functional segment unit (FSU) is more likely to be used in a kinematic study (**Figure 1**a). While in biomechanical tests, soft tissue, pedicles and posterior elements should also be removed (**Figure 1**b), and vertebral bodies can be embedded in polymetheylmethacrylata (PMMA) dental cement to ensure they are paralleled during the loading period. A separate disc without endplates can be used with external restrictions to prevent extrusion.

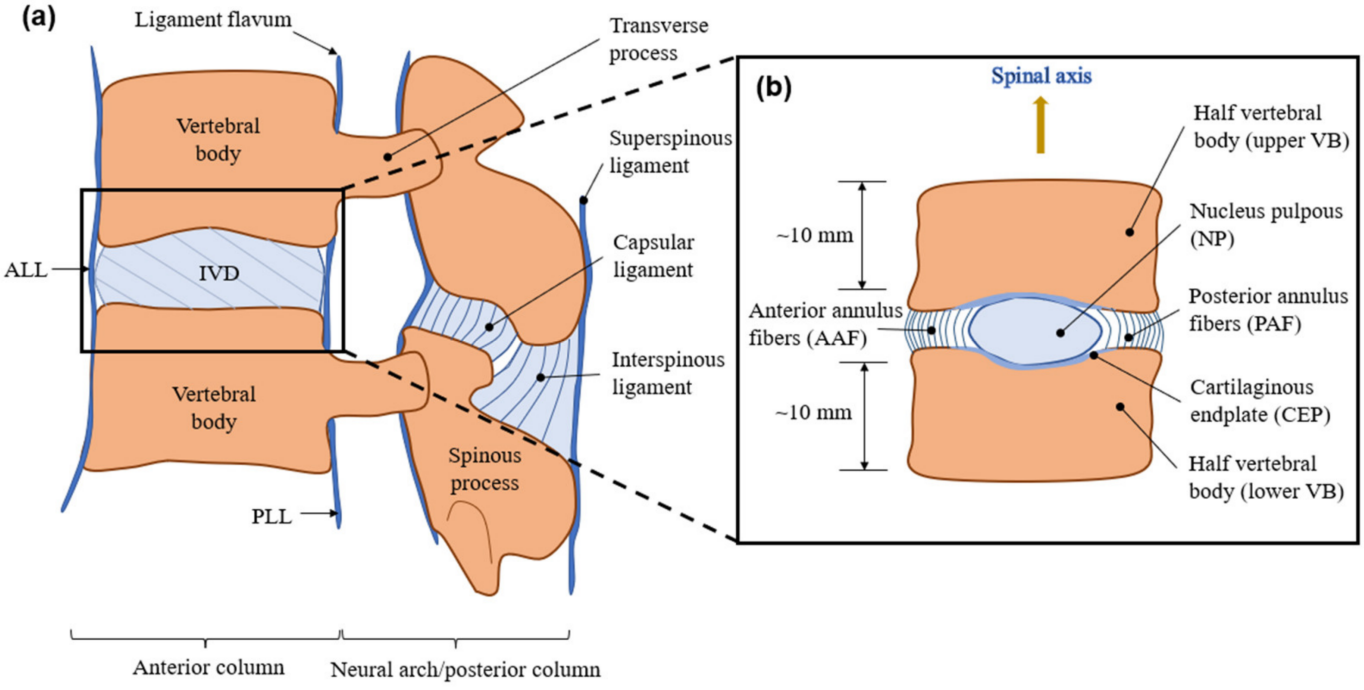

Figure 1. Schematic diagram of (**a**) functional spinal unit (FSU) (**b**) bone–disc–bone structure.

It should be noted that both vertebral bones and disc creep under prolonged constant loads. Although the creep of vertebral bones is tiny, several studies presented studies quantifying differences with or without bones. Schmidt performed a series of experiments [35][36] to compare the bone–disc–bone structure with the separate disc and demonstrated specific results with regard to displacement, stiffness and pressure under the same condition. The load regime included an 8 h preload under 0.06 MPa uniaxial compression, followed by 10 cycles of 10 min, in which the force was altered between 0.06 MPa and 0.5 MPa. Combined with the research of Oravec et al. [37], three types of specimen structures were used in total as follows: (1) a disc with endplates, (2) a disc without endplates and (3) an isolated vertebral body.

The disc contributed to the majority of the height loss during creep, and the bony endplates also exhibited significant impacts on the whole creep value (0.341 ± 0.269 mm under 1000 N after 2 h). Therefore, studies using bone–disc–bone specimens should exclude the height loss of vertebral bodies by appropriate methods of measurement in order to avoid larger and inaccurate results. It can be also seen that the stiffness of specimens with and without endplates was the same (700 N/mm). In the specimen without endplates, the intradiscal pressure was reduced by nearly 50% (~0.43 MPa). This may have contributed to the easy extrusion of the disc without circumferential constraints formed by the annulus and the bony structure, thus resulting in relatively unstable stress and a larger area of the cross-section. It is a reminder that a separate disc is an unsuitable structure in the study related to intradiscal pressure measurement.

Specimens for in vitro creep studies should be stored at −20 °C before testing. McMillan et al. [38] reported that, in case of inappropriate IVD storage (unloaded in a wet environment), swelling by 20% was noted due to the tension in the ligamentum flavum, generating pressure in NP for approximately 70 kPa [39]. Generally, a single freeze–thaw cycle exhibited minimal effects on the intradiscal pressure, stiffness, creep behavior of IVDs [40][41][42] and on the tensile property of AF [43]. However, after several freeze–thaw cycles, significant differences in the joint flexibility may occur [44], and several studies have reported mechanical differences between fresh and frozen IVDs [45][46]. To correct these differences, several studies verified that specimens immersed in saline solution or phosphate-buffered saline for more than 8 h prior to testing may be corrected for physiological hydration status [47].

2.3. Testing Environment

During experiments, hydration should be maintained to avoid the effects of dehydration by the following guidelines: (1) testing in a humidity chamber, (2) immersing in 0.15 M phosphate-buffered saline (PBS: 137 mM NaCl, 2.7 mM KCl, 5.4 mM Na2HPO4, and 0.6 mM KH2PO4) or saline solution (0.9% or 0.15 mol/L NaCl), or (3) wrapping in saline-soaked gauze [19]. The majority of studies immersed specimens in saline solutions during tests, while other studies placed specimens in the custom build culture system, in which the environment was kept at 37 °C with the presence of 5% CO2 [48][49], simulating the physiological conditions. To prevent infection, 10,000 u/mL penicillin, 250 mg/L streptomycin and 1.5 mg/mL amphoterizin B should be added in experiments lasting for more than 20 h [50]. A previous study focused on the influence of osmotic pressure on the fluid flow of IVDs with the change in concentration of PEG or NaCl [51]. Those studies conducted tests in the air [52][53] failed to maintain the hydration status, and their results should be treated dialectically.

Temperature is another factor that needs to be controlled. It was reported that body temperature at 37 °C could cause a 10% higher creep under compression than that at room temperature [54], while the results have not been confirmed by other studies.

2.4. Preload, Load Magnitudes and Duration

2.4.1. Preload

Prior to creep tests, preload is necessary for reaching physiological status and squeezing additional water. Moreover, it can prevent postmortem swelling, which often occurs on cadaveric IVDs [55]. The non-linear property of the IVDs suggests that stiffness can increase if a preload is applied prior to creep [56]. Therefore, the results of the experiments with the necessary preload period can be comparable. Although the duration of preload conditioning differed considerably, it was usually short before displacement equilibrium [34][57][58].

Typical forms of preload are 'static' and 'cyclic'. Generally, although certain studies incorporated thousands of pre-cycles [59], a static preload from 10 N to 50 N or three pre-cycles was sufficient for a consistent response of the IVDs [50].

2.4.2. Load Magnitude and Duration

Firstly, the load magnitude is of importance since disc height and intradiscal pressure are directly related [60][61]. Moreover, the strain in the annulus or bulge of the annulus fibrosus could be affected [62]. The magnitude of compressive force applied to the IVD varies in magnitude with changes in body posture, body weight, muscle activity and external loads [63][64][65]. In a study performed in eight healthy subjects, Nachemson and Morris et al. [66][67][68] demonstrated that the in vivo pressures in NP ranged from 0.091 MPa to 0.539 MPa when lying in prone or supine positions, from 0.46 MPa to 1.33 MPa in a seated position and from 0.5 MPa to 0.87 MPa in a standing position. Wilke et al. [61] reported that the highest pressure in the NP, 2.3 MPa, was recorded in a standing subject who was flexing forwards while simultaneously holding a 20 kg mass. These pressure values can be converted into corresponding load values by multiplying the area of the cross-section, which are ~100 N for L45 human IVDs during bedtime rest [20][36][60][61][69][70] and 750–1200 N during daytime activities. The loads for cervical spines are relatively lower than those for lumbar spines. For bovine tails (e.g., C23, C23), 27.7–209.1 N (0.06–0.28 MPa) and 211.6–373.4 N (~0.5 MPa) were simulated for loads of rest and daily activity [20][36][71]. For sheep lumbar, 40–60 N (~0.45 MPa) and 80–180 N (~1.05 MPa) were equal to nighttime unloading and daytime loading, respectively [34][60][72].

The representative loading regimes are shown in **Figure 2**, **Figure 3** and **Figure 4** and these can be divided into static, quasi-static and dynamic forms. Static load is the most simplified form of daily activities (e.g., sleep and sit) and is widely conducted in studies focusing on the mechanical properties of IVDs during creep. The quasi-static and dynamic loads are used to simulate the human body in physical exercise, driving and other daily activities. In addition, according to the frequencies of the vehicle under normal transportation conditions, the frequencies of vibration can be selected from 0 to 8 Hz in the dynamic creep experiments. Previous studies [73][74] suggested that, due to the resonant frequency of the human body, certain loading frequencies (4–6 Hz) may be harmful. **Table 3** summarizes the magnitudes and durations of preloads, loads and the major results from studies.

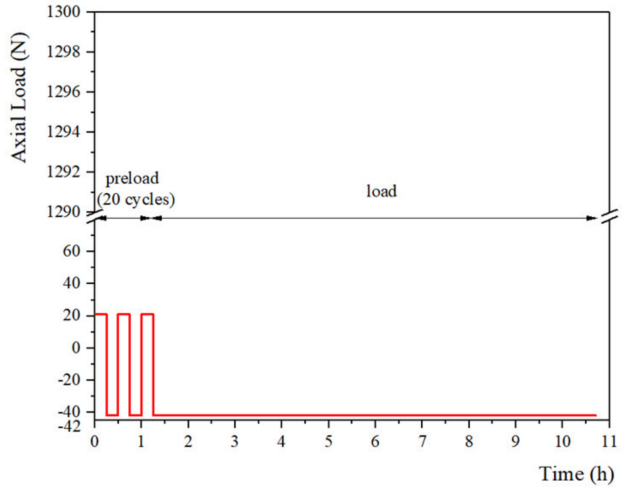
Axial Load (N)
preload
(20 cycles)
load
Time (h)

(a)

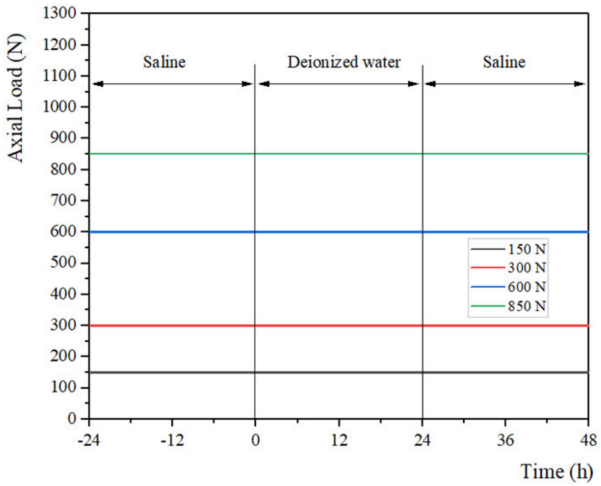
Axial Load (N)
Saline
Deionized water
Saline
150 N
300 N
600 N
850 N
Time (h)

(b)

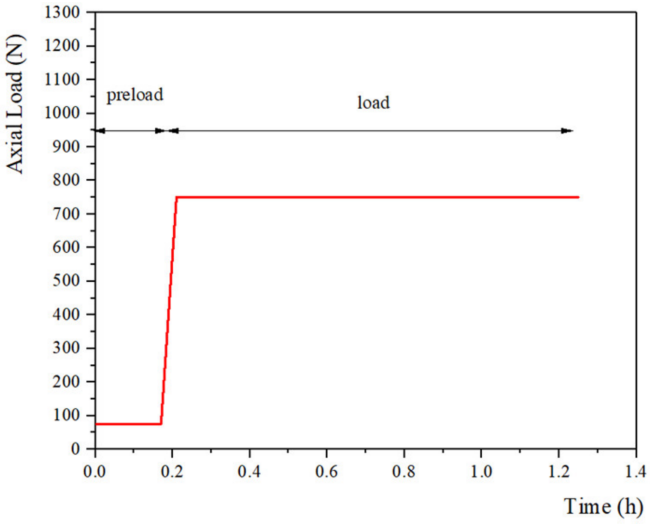
Axial Load (N)
preload
load
Time (h)

(c)

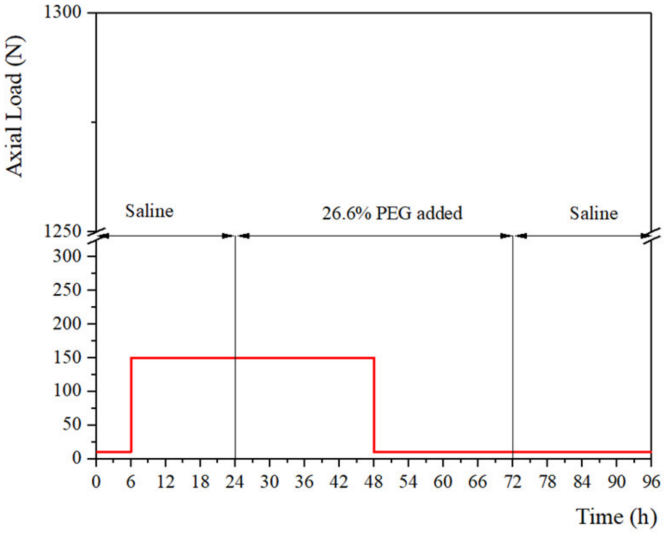
Axial Load (N)
Saline
26.6% PEG added
Saline
Time (h)

(d)

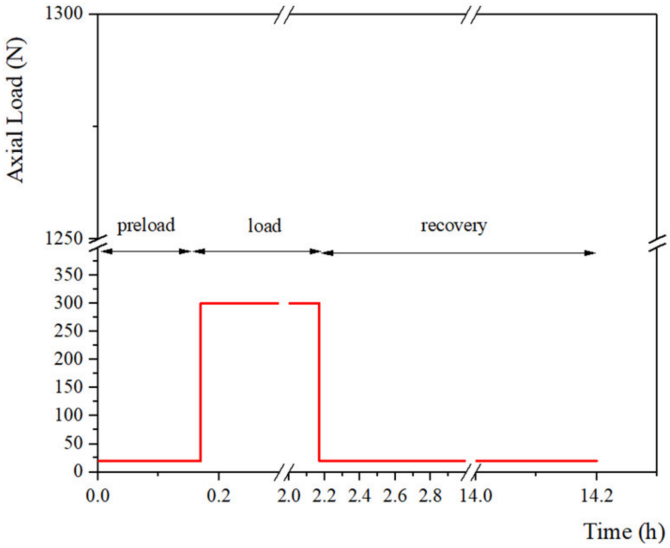
Axial Load (N)
preload
load
recovery
Time (h)

(e)

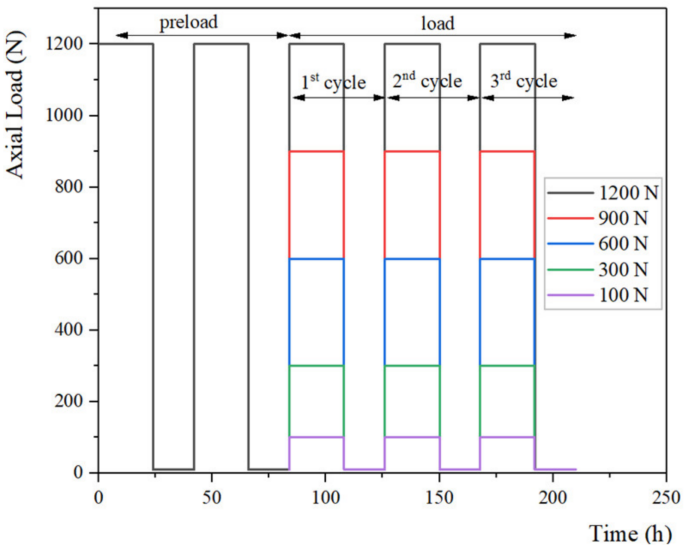
Axial Load (N)
preload
load
1st cycle
2nd cycle
3rd cycle
1200 N
900 N
600 N
300 N
100 N
Time (h)

(f)

Figure 2. Summary of loading regimes in the static creep experiments. The loading regimes from (**a**) Gullbrand et al. [75] conducted their test with 20 cycles of preload and a static load; (**b**) Vergroesen et al. [51] focused on the effects of the concentration change on creep behavior; (**c**) Hedman et al. [76] adopted both static preload and static load in the creep test; (**d**) Emanuel et al. [77] further studied the effects of changing solution on behaviors of IVDs; (**e**) Bezci et al. [71] paid attention to the height regaining process and the recovery time was longer; (**f**) Bezci et al. [78] conducted tests with static load and unload alternately.

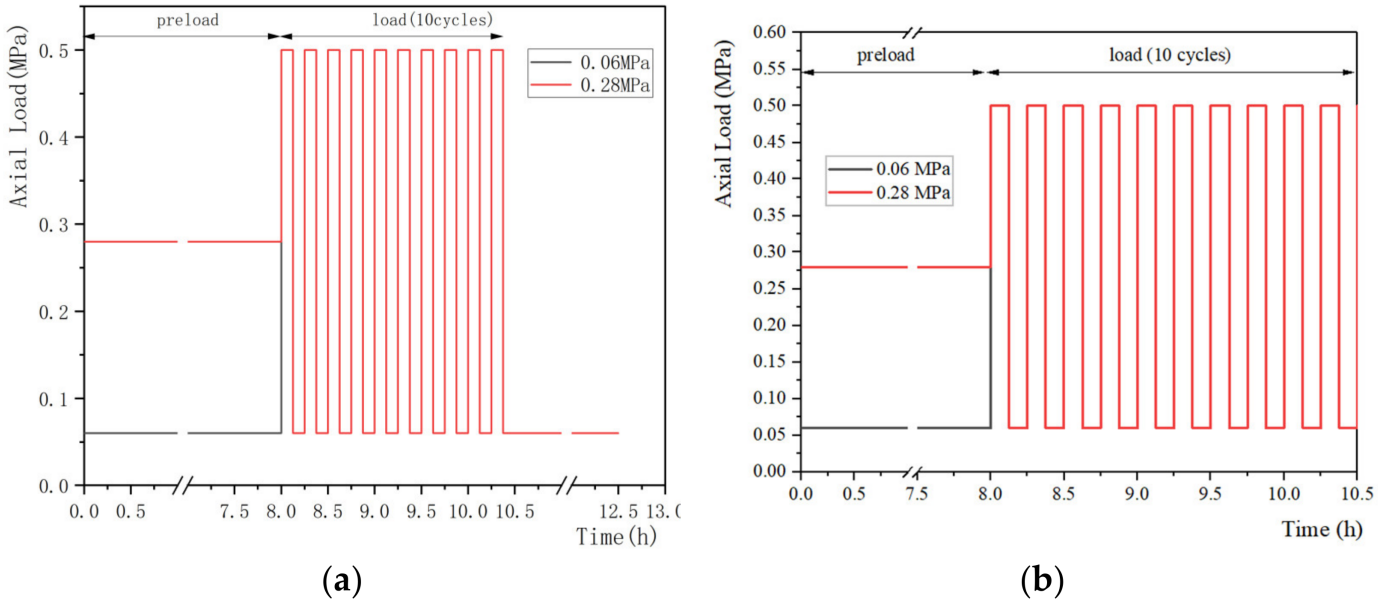

Figure 3. Summary of loading regimes in the quasi-static creep experiments, (**a**) Schmidt et al. [36] and (**b**) Schmidt et al. [35] conducted their test with a static preload and a quasi-static load.

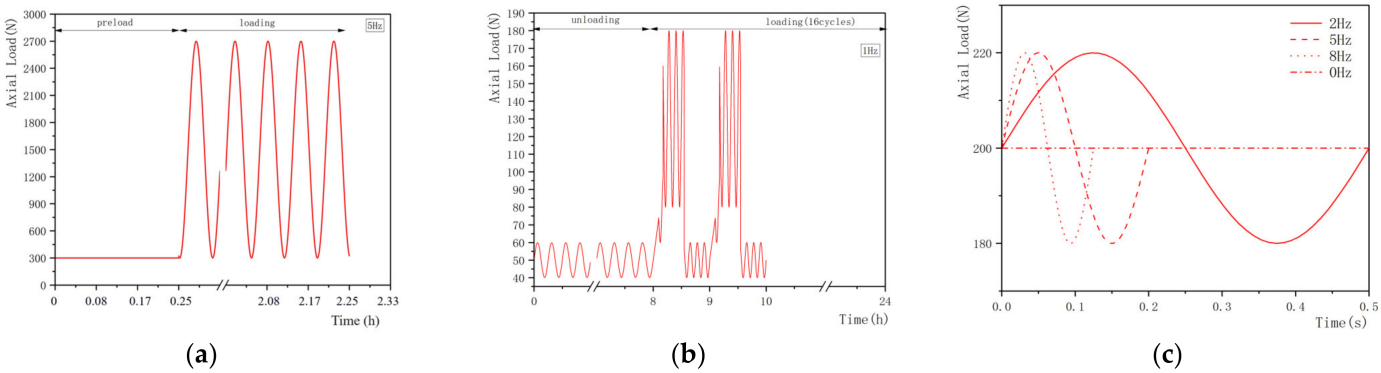

Figure 4. Summary of loading regimes in the dynamic creep experiments. The loading regimes from (**a**) Barrett et al. [79] were a static preload followed by a dynamic load; (**b**) Vergroesen et al. [72] conducted the dynamic test with several cycles of preload; (**c**) Yang et al. [80] conducted the dynamic test without preload.

Overview of preload, load and major results from in vitro creep tests. In cases where numerical values were not available, estimates were obtained from the figures. In cases where healthy and degenerate IVDs were tested, the

data from the healthy IVDs were recorded. In cases of more than one level of preload or load, the data refer to the highest value. Max. refers to ‘Maximum’. EP refers to ‘Endplate’. The references are listed in chronological order.

Secondly, the physiological condition, which is characterized by 8 h-preload and 16 h-load, can be shortened in the in vitro creep study. It has been shown that the measured displacement was more than 80% of the equilibrium displacement following creep for 4 h [47]. However, it should be noted that the creep behavior reached equilibrium within ~12 h [78] and that the time constant of human discs under creep was estimated at 14 h as reported by O’Connell et al. [47].

3. Selection of Loading Regime during Creep

3.1. Static Load

The static loads from 100 N to 1200 N are usually applied to simulate the diurnal load from the aggregated literature [51][71][75][76][78]. The large range of the selected loads is mainly due to significant differences in the area of cross-section of the specimens used in studies. Moreover, it should also correspond to the physiological conditions of the species according to published in vivo studies. The selection of the duration varied from 10 min to 24 h. Some studies conducted tests for 12–24 h to simulate responses of IVDs diurnally [51][75]; other studies even lasted for several days and were thought to be time-consuming [78]; the reduction to 10 min may be too short to explore the creep behaviors [77]. A previous study indicated that the majority of the equilibrium displacement (>80%) occurred within 4 h [47], and the duration of their creep study was also 4 h, leading to the advice that the duration of 4 h was suitable to reduce the time cost.

3.2. Quasi-Static Load

The forces in the quasi-static creep experiments are alternated with high and low loads with a certain interval. The loading regimes in **Figure 3** are typical quasi-static patterns, which contain more than 10 cycles of 15 min, including a high load (~0.5 MPa) and a low load (~0.06 or 0.28 MPa) in a cycle. This enables the simulation of the behaviors of the IVDs under loads with frequencies in daily activities. The quasi-static load always lasts for 2–4 h to replicate the in vivo status of the daytime loading period.

3.3. Dynamic Load

Dynamic loading regimes can be used to replicate the creep response of IVDs under various physiological frequencies. According to the range of frequency of daily activities (e.g., doing sports or driving), it could be selected from 0 to 8 Hz to simulate the in vivo conditions [80]. In the study from Barrett et al. [79], the mean force of sinusoidal load was 1500 N (**Figure 4**), which was relatively higher than that of the physiological loads. 130 N and 200 N were used in the studies of Vergroessen et al. [72] and Yang et al. [80] which were considered as rationally based on physiology.

References

1. Twomey, L.; Taylor, J. Flexion Creep Deformation and Hysteresis in the Lumbar Vertebral Column. Spine 1982, 7, 116–122.
2. Koeller, W.; Funke, F.; Hartmann, F.; Copley, A.L.; Witte, S. Biomechanical behavior of human intervertebral discs subjected to log lasting axial loading. Biorheology 1984, 21, 675–686.
3. Leatt, P.; Reilly, T.; Troup, J.G. Spinal loading during circuit weight-training and running. Br. J. Sports Med. 1986, 20, 119–124.
4. Pollintine, P.; Tunen, M.V.; Luo, J.; Brown, M.D.; Dolan, P.; Adams, M.A. Time-dependent Compressive Deformation of the Ageing Spine: Relevance to Spinal Stenosis. Spine 2010, 35, 386–394.
5. Adams, M.; Hutton, W.C. The Effect of Posture on the Fluid Content of Lumbar Intervertebral Discs. Spine 1983, 8, 665–671.
6. Adams, M.A.; Dolan, P. Time-dependent changes in the lumbar spine’s resistance to bending. Clin. Biomech. 1996, 11, 194–200.
7. Brown, T.; Hansen, R.J.; Yorra, A.J. Some mechanical tests on the lumbosacral spine with particular reference to the intervertebral discs: A preliminary report. J. Bone Jt. Surg. Am. 1957, 39-A, 1135–1164.
8. Burns, M.L.; Kaleps, I.; Kazarian, L.E. Analysis of compressive creep behavior of the vertebral unit subjected to a uniform axial loading using exact parametric solution equations of Kelvin-solid models—Part I. Human intervertebral joints. J. Biomech. 1984, 17, 113–130.
9. Hirsch, C. The Reaction of Intervertebral Discs to Compression Forces. J. Bone Jt. Surg. 1955, 37, 1188–1196.
10. Hirsch, C.; Nachemson, A. New observations on the mechanical behavior oflumbar discs. Acta Orthop. Scand. 1994, 23, 254–283.
11. Kazarian, L.E. Creep Characteristics of the Human Spinal Column. Orthop. Clin. N. Am. 1975, 6, 3–18.
12. Koeller, W.; Meier, W.; Hartmann, F. Biomechanical properties of human intervertebral discs subjected to axial dynamic compression. A comparison of lumbar and thoracic discs. Spine 1984, 9, 725–733.
13. Kulak, R.F.; Schultz, A.B.; Belytschko, T.; Galante, J. Biomechanical characteristics of vertebral motion segments and inter-vertebral disks. Orthop. Clin. N. Am. 1975, 6, 121–133.
14. Lin, H.; Lui, Y.K.; Ray, G.; Nikravesh, P. Systems identification for material properties of the intervertebral joint. J. Biomech. 1978, 11, 1–14.

15. Lin, L.-C.; Hedman, T.P.; Wang, S.-J.; Huoh, M.; Chuang, S.-Y. The Analysis of Axisymmetric Viscoelasticity, Time-Dependent Recovery, and Hydration in Rat Tail Intervertebral Discs by Radial Compression Test. J. Appl. Biomech. 2009, 25, 133–139.
16. Markolf, K.L. Deformation of the thoracolumbar intervertebral joints in response to external loads: A biomechanical study using autopsy material. J. Bone Jt. Surg. 1972, 54, 511–533.
17. Virgin, W.J. Experimental investigations into the physical properties of the intervertebral disc. J. Bone Jt. Surg. Br. 1951, 33, 607–611.
18. Schmidt, H.; Reitmaier, S.; Graichen, F.; Shirazi-Adl, A. Review of the fluid flow within intervertebral discs—How could in vitro measurements replicate in vivo? J. Biomech. 2016, 49, 3133–3146.
19. Newell, N.; Little, J.P.; Christou, A.; Adams, M.A.; Adam, C.J.; Masouros, S.D. Biomechanics of the Human Intervertebral Disc: A Review of Testing Techniques and Results. J. Mech. Behav. Biomed. Mater. 2017, 69, 420–434.
20. O'Connell, G.D.; Vresilovic, E.J.; Elliott, D.M. Comparison of animals used in disc research to human lumbar disc geometry. Spine 2007, 32, 328–333.
21. Kuo, Y.-W.; Wang, J.-L. Rheology of Intervertebral Disc. Spine 2010, 35, E743–E752.
22. Ishihara, H.; Tsuji, H.; Hirano, N.; Ohshirna, H.; Terahata, N. Biorheological responses of the intact and nucleotomized in-tervertebral discs to compressive, tensile, and vibratory stresses. Clin. Biomech. 1993, 8, 250–254.
23. Beckstein, J.C.; Sen, S.; Schaer, T.P.; Vresilovic, E.J.; Elliott, D.M. Comparison of animal discs used in disc research to human lumbar disc: Axial compression mechanics and glycosaminoglycan content. Spine 2008, 33, E166–E173.
24. Gooyers, C.E.; McMillan, R.D.; Howarth, S.J.; Callaghan, J.P. The Impact of Posture and Prolonged Cyclic Compressive Loading on Vertebral Joint Mechanics. Spine 2012, 37, E1023–E1029.
25. Iatridis, J.C.; Laible, J.P.; Krag, M.H. Influence of Fixed Charge Density Magnitude and Distribution on the Intervertebral Disc: Applications of a Poroelastic and Chemical Electric (PEACE) Model. J. Biomech. Eng. 2003, 125, 12–24.
26. Boxberger, J.I.; Sen, S.; Yerramalli, C.S.; Elliott, D.M. Nucleus pulposus glycosaminoglycan content is correlated with axial mechanics in rat lumbar motion segments. J. Orthop. Res. 2006, 24, 1906–1915.
27. Johannessen, W.; Elliott, D.M. Effects of degeneration on the biphasic material properties of human nucleus pulposus in con-fined compression. Spine 2005, 30, E724–E729.

28. Demers, C.N.; Antoniou, J.; Mwale, F. Value and Limitations of Using the Bovine Tail as a Model for the Human Lumbar Spine. Spine 2004, 29, 2793–2799.
29. Antoniou, J.; Steffen, T.; Nelson, F.; Winterbottom, N.; Hollander, A.P.; Poole, R.A.; Aebi, M.; Alini, M. The human lumbar intervertebral disc: Evidence for changes in the biosynthesis and denaturation of the extracellular matrix with growth, maturation, ageing, and degeneration. J. Clin. Investig. 1996, 98, 996–1003.
30. Urban, J.P.; McMullin, J.F. Swelling pressure of the intervertebral disc: Influence of proteoglycan and collagen contents. Biorheology 1985, 22, 145–157.
31. Yates, J.P.; Giangregorio, L.; McGill, S.M. The Influence of Intervertebral Disc Shape on the Pathway of Posterior/Posterolateral Partial Herniation. Spine 2010, 35, 734–739.
32. Van Heeswijk, V.M.; Thambyah, A.; Robertson, P.A.; Broom, N.D. Posterolateral disc prolapse in flexion initiated by lateral inner annular failure: An investigation of the herniation pathway. Spine 2017, 42, 1604–1613.
33. Alini, M.; Eisenstein, S.M.; Ito, K.; Little, C.; Kettler, A.A.; Masuda, K.; Melrose, J.; Ralphs, J.; Stokes, I.; Wilke, H.J. Are animal models useful for studying human disc disorders/degeneration? Eur. Spine J. 2007, 17, 2–19.
34. Reitmaier, S.; Schmidt, H.; Ihler, R.; Kocak, T.; Graf, N.; Ignatius, A.; Wilke, H.-J. Preliminary Investigations on Intradiscal Pressures during Daily Activities: An In Vivo Study Using the Merino Sheep. PLoS ONE 2013, 8, e69610.
35. Schmidt, H.; Shirazi-Adl, A.; Schilling, C.; Dreischarf, M. Preload substantially influences the intervertebral disc stiffness in loading–unloading cycles of compression. J. Biomech. 2016, 49, 1926–1932.
36. Schmidt, H.; Schilling, C.; Reyna, A.L.P.; Shirazi-Adl, A.; Dreischarf, M. Fluid-flow dependent response of intervertebral discs under cyclic loading: On the role of specimen preparation and preconditioning. J. Biomech. 2016, 49, 846–856.
37. Oravec, D.; Kim, W.; Flynn, M.J.; Yeni, Y.N. The relationship of whole human vertebral body creep to geometric, microstructural, and material properties. J. Biomech. 2018, 73, 92–98.
38. McMillan, D.W.; Garbutt, G.; Adams, M.A. Effect of sustained loading on the water content of intervertebral discs: Implications for disc metabolism. Ann. Rheum. Dis. 1996, 55, 880–887.
39. Heuer, F.; Schmidt, H.; Klezl, Z.; Claes, L.; Wilke, H.-J. Stepwise reduction of functional spinal structures increase range of motion and change lordosis angle. J. Biomech. 2007, 40, 271–280.
40. Dhillon, N.; Bass, E.C.; Lotz, J.C. Effect of Frozen Storage on the Creep Behavior of Human Intervertebral Discs. Spine 2001, 26, 883–888.

41. Panjabi, M.M.; Krag, M.; Summers, D.; Videman, T. Biomechanical time-tolerance of fresh cadaveric human spine specimens. J. Orthop. Res. 1985, 3, 292–300.
42. Smeathers, J.E.; Joanes, D.N. Dynamic compressive properties of human lumbar intervertebral joints: A comparison between fresh and thawed specimens. J. Biomech. 1988, 21, 425–433.
43. Galante, J.O. Tensile properties of the human lumbar annulus fibrosus. Acta Orthop. Scand. Suppl. 1967, 100, 1–91.
44. Tan, J.S.; Uppuganti, S. Cumulative multiple freeze-thaw cycles and testing does not affect subsequent within-day variation in intervertebral flexibility of human cadaveric lumbosacral spine. Spine 2012, 37, E1238–E1242.
45. Callaghan, J.P.; McGill, S.M. Frozen storage increases the ultimate compressive load of porcine vertebrae. J. Orthop. Res. 1995, 13, 809–812.
46. Sunni, N.; Askin, G.N.; Labrom, R.D.; Izatt, M.T.; Pearcy, M.J.; Adam, C.J. The effect of repeated loading and freeze-thaw cycling on immature bovine thoracic motion segment stiffness. Proc. Inst. Mech. Eng. Part H J. Eng. Med. 2014, 228, 1100–1107.
47. O'Connell, G.D.; Jacobs, N.T.; Sen, S.; Vresilovic, E.J.; Elliott, D.M. Axial creep loading and unloaded recovery of the human intervertebral disc and the effect of degeneration. J. Mech. Behav. Biomed. Mater. 2011, 4, 933–942.
48. Paul, C.P.L.; Schoorl, T.; Zuiderbaan, H.A.; ZandiehDoulabi, B.; van der Veen, A.J.; van de Ven, P.M.; Smit, T.H.; van Royen, B.J.; Helder, M.N.; Mullender, M.G. Dynamic and Static Overloading Induce Early Degenerative Processes in Caprine Lumbar Intervertebral Discs. PLoS ONE 2013, 8, e62411.
49. Paul, C.P.L.; Zuiderbaan, H.A.; ZandiehDoulabi, B.; van der Veen, A.J.; van de Ven, P.M.; Smit, T.H.; Helder, M.N.; van Royen, B.J.; Mullender, M.G. Simulated-physiological loading conditions preserve biological and mechanical properties of caprine lumbar intervertebral discs in ex vivo culture. PLoS ONE 2012, 7, e33147.
50. Wilke, H.-J.; Wenger, K.; Claes, L. Testing criteria for spinal implants: Recommendations for the standardization of in vitro stability testing of spinal implants. Eur. Spine J. 1998, 7, 148–154.
51. Vergroesen, P.; van der Veen, A.; Emanuel, K.S.; van Dieën, J.V.; Smit, T.H. The poro-elastic behaviour of the intervertebral disc: A new perspective on diurnal fluid flow. J. Biomech. 2016, 49, 857–863.
52. Ingelmark, B.E.; Ekholm, R. The compressibility of intervertebral disks: An experimental investigation on the intervertebral disk between the third and fourth lumbar vertebrae in man. Acta Soc. Med. Ups. 1952, 57, 202–217.

53. Brinckmann, P.; Horst, M. The influence of vertebral body fracture, intradiscal injection, and partial discectomy on the radial bulge and height of human lumbar discs. Spine 1985, 10, 138–145.
54. Koeller, W.; Muehlhaus, S.; Meier, W.; Hartmann, F. Biomechanical properties of human intervertebral discs subjected to axial dynamic compression—Influence of age and degeneration. J. Biomech. 1986, 19, 807–816.
55. Parkinson, R.J.; Durkin, J.L.; Callaghan, J.P. Estimating the Compressive Strength of the Porcine Cervical Spine: An Examination of the Utility of DXA. Spine 2005, 30, E492–E498.
56. Janevic, J.; Ashton-Miller, J.A.; Schultz, A.B. Large compressive preloads decrease lumbar motion segment flexibility. J. Orthop. Res. 1991, 9, 228–236.
57. Van der Veen, A.J.; Mullender, M.; Smit, T.H.; Kingma, I.; van Dieën, J.H. Flow-Related Mechanics of the Intervertebral Disc: The Validity of an In Vitro Model. Spine 2005, 30, E534–E539.
58. Van der Veen, A.J.; Mullender, M.G.; Kingma, I.; van Dieen, J.H.; Smit, T.H. Contribution of vertebral bodies, endplates, and in-tervertebral discs to the compression creep of spinal motion segments. J. Biomech. 2008, 41, 1260–1268.
59. Costi, J.; Heinze, K.; Lawless, I.; Stanley, R.; Freeman, B. Do combined compression, flexion and axial rotation place degenerated discs at risk of posterolateral herniation? Measurement of 3D lumbar intervertebral disc internal strains during repetitive loading. Bone Jt. J. Orthop. Proc. Suppl. 2014, 96-B, 219.
60. Vergroesen, P.-P.A.; Van Der Veen, A.J.; Van Royen, B.J.; Kingma, I.; Smit, T.H. Intradiscal pressure depends on recent loading and correlates with disc height and compressive stiffness. Eur. Spine J. 2014, 23, 2359–2368.
61. Wilke, H.; Neef, P.; Caimi, M.; Hoogland, T.; Claes, L.E. New In Vivo Measurements of Pressures in the Intervertebral Disc in Daily Life. Spine 1999, 24, 755–762.
62. Brinckmann, P.; Grootenboer, H. Change of Disc Height, Radial Disc Bulge, and Intradiscal Pressure from Discectomy An in Vitro Investigation on Human Lumbar Discs. Spine 1991, 16, 641–646.
63. Callaghan, J.P.; Gunning, J.L.; McGill, S.M. The relationship between lumbar spine load and muscle activity during extensor exercises. Phys. Ther. 1998, 78, 8–18.
64. Han, K.-S.; Rohlmann, A.; Zander, T.; Taylor, W.R. Lumbar spinal loads vary with body height and weight. Med. Eng. Phys. 2013, 35, 969–977.
65. Nachemson, A.L. Disc Pressure Measurements. Spine 1981, 6, 93–97.
66. Nachemson, A.; Morris, J.M. In Vivo Measurements of Intradiscal Pressure. J. Bone Jt. Surg. 1964, 46, 1077–1092.

67. Nachemson, A.; Morris, J. Lumbar discometry lumbar intradiscal pressure Page 37 of 55 measurements in vivo. Lancet 1963, 281, 1140–1142.
68. Sato, K.; Kikuchi, S.; Yonezawa, T. In Vivo Intradiscal Pressure Measurement in Healthy Individuals and in Patients with Ongoing Back Problems. Spine 1999, 24, 2468–2474.
69. Dreischarf, M.; Shirazi-Adl, A.; Arjmand, N.; Rohlmann, A.; Schmidt, H. Estimation of loads on human lumbar spine: A review of in vivo and computational model studies. J. Biomech. 2016, 49, 833–845.
70. Ferguson, S.J.; Ito, K.; Nolte, L.-P. Fluid flow and convective transport of solutes within the intervertebral disc. J. Biomech. 2004, 37, 213–221.
71. Bezci, S.E.; O'Connell, G.D. Osmotic Pressure Alters Time-dependent Recovery Behavior of the Intervertebral Disc. Spine 2018, 43, E334–E340.
72. Vergroesen, P.-P.A.; Emanuel, K.S.; Peeters, M.; Kingma, I.; Smit, T.H. Are axial intervertebral disc biomechanics determined by osmosis? J. Biomech. 2018, 70, 4–9.
73. Wilder, D.; Pope, M. Epidemiological and aetiological aspects of low back pain in vibration environments—An update. Clin. Biomech. 1996, 11, 61–73.
74. Kumar, A.; Varghese, M.; Mohan, D.; Mahajan, P.; Gulati, P.; Kale, S. Effect of whole-body vibration on the low back. A study of tractor-driving farmers in north India. Spine 1999, 24, 2506–2515.
75. Gullbrand, S.E.; Ashinsky, B.G.; Martin, J.T.; Pickup, S.; Smith, L.J.; Mauck, R.L.; Smith, H.E. Correlations between quantitative T 2 and T 1ρ MRI, mechanical properties and biochemical composition in a rabbit lumbar intervertebral disc degeneration model. J. Orthop. Res. 2016, 34, 1382–1388.
76. Hedman, T.P.; Chen, W.-P.; Lin, L.-C.; Lin, H.-J.; Chuang, S.-Y. Effects of Collagen Crosslink Augmentation on Mechanism of Compressive Load Sharing in Intervertebral Discs. J. Med. Biol. Eng. 2017, 37, 94–101.
77. Emanuel, K.S.; van der Veen, A.J.; Rustenburg, C.M.; Smit, T.H.; Kingma, I. Osmosis and viscoelasticity both contribute to time-dependent behaviour of the intervertebral disc under compressive load: A caprine in vitro study. J. Biomech. 2018, 70, 10–15.
78. Bezci, S.E.; Lim, S.; O'Connell, G.D. Nonlinear stress-dependent recovery behavior of the intervertebral disc. J. Mech. Behav. Biomed. Mater. 2020, 110, 103881.
79. Barrett, J.M.; Gooyers, C.E.; Karakolis, T.; Callaghan, J.P. The Impact of Posture on the Mechanical Properties of a Functional Spinal Unit During Cyclic Compressive Loading. J. Biomech. Eng. 2016, 138, 081007.

80. Yang, X.; Cheng, X.; Luan, Y.; Liu, Q.; Zhang, C. Creep experimental study on the lumbar intervertebral disk under vibration compression load. Proc. Inst. Mech. Eng. Part H J. Eng. Med. 2019, 233, 858–867.